Clinical Biomechanics 29 (2014) 451–457

Contents lists available at ScienceDirect

Clinical Biomechanics

journal homepage: www.elsevier.com/locate/clinbiomech

Geometrical adaptation in ulna and radius of cerebral palsy patients: Measures and consequences

M. de Bruin [a,*], M. van de Giessen [b,c], J.C. Vroemen [a], H.E.J. Veeger [d,e], M. Maas [f], S.D. Strackee [a], M. Kreulen [a,g]

[a] *Department of Plastic, Reconstructive, and Hand Surgery, Academic Medical Center, Amsterdam, The Netherlands*
[b] *Department of Radiology, Leiden University Medical Center, Leiden, The Netherlands*
[c] *Department of Intelligent Systems, Faculty of Electrical Engineering, Applied Mathematics and Computer Science, Delft University of Technology, Delft, The Netherlands*
[d] *Research Institute MOVE, Faculty of Human Movement Sciences, VU University, Amsterdam, The Netherlands*
[e] *Section Biomechatronics & Biorobotics, Faculty of Material Sciences, Delft University of Technology, Delft, The Netherlands*
[f] *Department of Radiology, Academic Medical Center, Amsterdam, The Netherlands*
[g] *Department of Plastic, Reconstructive, and Hand Surgery, Red Cross Hospital, Beverwijk, The Netherlands*

ARTICLE INFO

Article history:
Received 11 January 2013
Accepted 6 January 2014

Keywords:
Cerebral palsy
Bone deformity
Spasticity
Potential maximal moment

ABSTRACT

Background: The presence of significant forearm bone torsion might affect planning and evaluating treatment regimes in cerebral palsy patients. We aimed to evaluate the influence of longstanding wrist flexion, ulnar deviation, and forearm pronation due to spasticity on the bone geometries of radius and ulna. Furthermore, we aimed to model the hypothetical influence of these deformities on potential maximal moment balance for forearm rotation.

Methods: Geometrical measures were determined in hemiplegic cerebral palsy patients ($n = 5$) and healthy controls ($n = 5$). Bilateral differences between the spastic arm and the unaffected side were compared to bilateral differences between the dominant and non-dominant side in the healthy controls. Hypothetical effects of bone torsion on potential maximal forearm rotation moment were calculated using an existing anatomical muscle model.

Findings: Patients showed significantly smaller (radius: 41.6%; ulna: 32.9%) and shorter (radius: 9.1%; ulna: 8.4%) forearm bones in the non-dominant arm than in the dominant arm compared to controls (radius: 2.4%; ulna 2.5% and radius: 1.5%; ulna: 1.0% respectively). Furthermore, patients showed a significantly higher torsion angle difference (radius: 24.1°; ulna: 26.2°) in both forearm bones between arms than controls (radius: 2.0°; ulna 1.0°). The model predicted an approximate decrease of 30% of potential maximal supination moment as a consequence of bone torsion.

Interpretation: Torsion in the bones of the spastic forearm is likely to influence potential maximal moment balance and thus forearm rotation function. In clinical practice, bone torsion should be considered when evaluating movement limitations especially in children with longstanding spasticity of the upper extremity.

1. Introduction

Hemiplegic cerebral palsy of the spastic type (CP) presents with a developmental disorder of movement and posture causing activity limitations that are attributed to non-progressive disturbances that occurred in the developing fetal or infant brain (Bax et al., 2005; Mutch et al., 1992). CP patients typically present with awkward movement patterns that highly affect arm–hand function during functional tasks (Donkervoort et al., 2007; Livingston et al., 2011). Although the exact cause of movement limitations in the spastic arm is unknown, adaptations in soft tissue due to constant pathological loads on the muscles seem to play a role (de Bruin et al., 2013). Although studies on malalignment of the radius suggest that bone deformities result in decreased functionality of the wrist (McQueen and Caspers, 1988), possible forearm bone deformities as a result of spasticity in CP patients and the hypothetical consequences for arm function have to our knowledge not been described.

Shape parameters of the non-pathological forearm bones are considered naturally optimal for functional pronation–supination motion (Allaire et al., 2003). However, according to Wolff's Law, bone adapts to mechanical loading (Daly et al., 2004; Whiteley et al., 2009). Bilateral morphological differences between bones of the dominant and non-preferred arm in tennis players (Bass et al., 2002; Ducher et al., 2006), baseball pitchers (Sabick et al., 2005; Warden et al., 2009), brachial plexus palsy patients (Hoeksma et al., 2003) and CP patients (Demir et al., 2006) confirm this law. Moreover, the effect of exercise on bone growth has been shown to be greater if exercise has started before

* Corresponding author at: Department of Plastic, Reconstructive, and Hand Surgery, Academic Medical Center, Postbox 22660, Suite G4-226, 1100 DD Amsterdam, The Netherlands.
E-mail address: marijedebruin@gmail.com (M. de Bruin).

0268-0033/$ – see front matter © 2014 Elsevier Ltd. All rights reserved.
http://dx.doi.org/10.1016/j.clinbiomech.2014.01.003

Table 1
Patient characteristics (Gschwind and Tonkin, 1992; Zancolli et al., 1987).

Subject	Age	Spastic arm	Zancolli[a] grasp and release pattern	Gschwind[b] pronation deformity
1	21	Right	III	3
2	34	Left	IIB	4
3	35	Right	IIB	3
4	27	Right	IIB	3
5	23	Left	IIB	2

[a] Wrist flexion deformity during grasp and release according to Zancolli et al., 1987.
[b] Pronation deformity according to Gschwind and Tonkin, 1992.

puberty (Kannus et al., 1995). Furthermore, arm length discrepancy in CP has been shown to increase with age and to be related to hand function, but not to spasticity (Demir et al., 2006). A change in the geometry of the bones will cause shifts of relative muscle attachment sites resulting in changes in muscle moment arms. Consequently, the potential maximal moment (PMM) of several muscles and thus the PMM balance for each joint angle will change (Ettema et al., 1998; Veeger et al., 2004).

We aimed to study the influence of longstanding wrist flexion, ulnar deviation and forearm pronation due to CP on forearm bone growth and on the development of torsion in the radius and ulna by describing bilateral symmetry of the forearm bones (Vroemen et al., 2012). Furthermore, we aimed to describe the effect of the supposed changes in geometry on forearm rotation function of the spastic arm. For this, we compared computed tomography (CT) scan-based three-dimensional reconstructions of the spastic forearm to the contralateral, unaffected forearm in patients with CP.

It was expected that the radius, but not the ulna, will show a pronated orientation relative to the contralateral forearm and that the affected forearm will have a smaller volume than the contralateral unaffected forearm. These differences were expected to be significantly larger in patients than in healthy controls, for which no, or only minimal, differences are expected. This information will help understanding movement disorders in this patient group and potentially improve treatment.

2. Methods

2.1. Subjects

Five adult subjects (mean age 28, range 21–35 years) with spastic hemiplegic CP and five adult control subjects (mean age 25, range 23–31 years) were included for comparison of bilateral differences between groups. Patient characteristics are described in Table 1, the right arm was the dominant arm for all control subjects. The spastic arm will from now on be referred to as the non-dominant arm. All subjects gave written informed consent before the start of the study, which was approved by the local Medical Ethics Committee (NL38330.018.11). The study adhered to the ethical guidelines of the 1975 Declaration of Helsinki.

2.2. CT scans/imaging

One regular-dose, high-resolution CT scan of each forearm was obtained using standardized clinical methods (Philips Brilliance 64 CT scanner, Cleveland, OH; voxel size 0.33 × 0.33 × 0.33 mm, 120 kV, 150 mAs, pitch 0.6; 0.6 mSv). Interpolation was done by the CT-scan itself. The original voxel sizes were kept unchanged between scans.

Scans were segmented semi-automatically using in-house developed software that uses a region-growing algorithm to extract the bone surfaces. In each subject, the radii and ulnae were segmented by threshold-connected region growing, followed by a binary closing algorithm for filling residual holes and closing of the outline (Dobbe et al., 2011). We derived a three-dimensional polygon from the segmented data that served as a virtual three-dimensional model of the bone. Surfaces of radius and ulna were obtained using Marching Cubes (Lorensen and Cline, 1987) as implemented in MATLAB® (The Mathworks, Natick, MA, USA). Volumes were calculated by counting the number of voxels within the bone segmentations, multiplied by the voxel volume. The large segmented volume, compared to the segmented surface, warrants that errors due to voxelwise counting are negligible in this data.

2.3. Torsion and bending estimates

Left side bones were mirrored to right side bones. Torsions of the radii and ulnae were determined with respect to the principal axes of the radius and ulna. These axes were estimated using principal component analysis (Webb, 2002) on the points that constitute the triangulated surface as extracted by the Marching Cubes method. Subsequently, the radii and ulnae were aligned by alternatively estimating the most likely point-to-point correspondences between the dominant and non-dominant bone models and rigidly aligning these until convergence while allowing for scaling. The expectation–maximization iterative closest point method (EM–ICP method; Granger and Pennec, 2002) was used, a variation of the ICP algorithm that is less sensitive to local minima and thereby results in more accurate registrations. Subsequently, the proximal 20% and distal 20% of the non-dominant bone models were registered to the contralateral side using the EM–ICP method with scaling. The torsion angle was then determined for the distal end with respect to the proximal end around the principal bone axis of the unaffected bone model (Fig. 1). Positive angles indicate torsion towards pronation and negative angles torsion towards

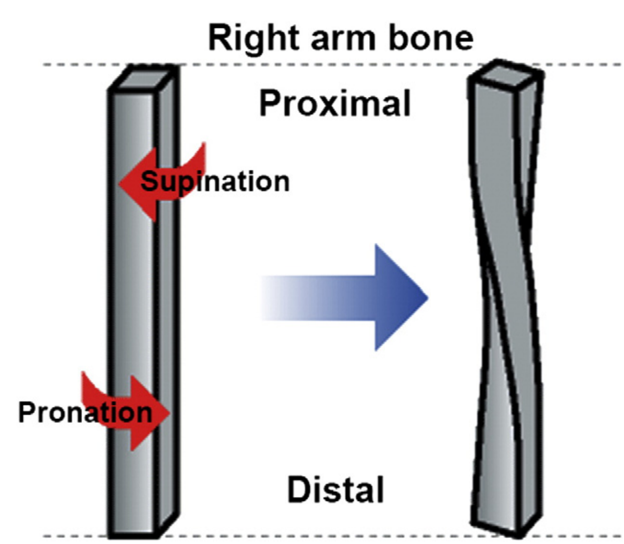

Fig. 1. Schematic drawing of torsion, where the distal end moves towards pronation and the proximal end moves towards supination.